Cell Cycle 10:2, 308-322; January 15, 2011; © 2011 Landes Bioscience

KAP1 depletion increases PML nuclear body number in concert with ultrastructural changes in chromatin

Rosemarie Kepkay,[1] Kathleen M. Attwood,[1] Yael Ziv,[2] Yosef Shiloh[2] and Graham Dellaire[1,3,*]

[1]Departments of Pathology and Biochemistry and Molecular Biology; Dalhousie University; [3]Beatrice Hunter Cancer Research Institute; Halifax, NS, Canada;
[2]Department of Human Molecular Genetics and Biochemistry; Sackler School of Medicine; Tel Aviv University; Tel Aviv, Israel

Key words: PML nuclear bodies, KAP1, DNA repair, chromatin structure, electron microscopy

Abbreviations: ATM, ataxia telangiectasia mutated; ATR, ATM and Rad3-related; DSB, double-strand break; HDAC, histone deacetylase; KAP1, KRAB-associated protein 1; NHDF, normal human diploid fibroblasts; PIKK, phosphatidyl-inositol 3-kinase; PML NB, promyelocytic leukemia nuclear bodies; topo II, topoisomerase II; TSA, trichostatin A; WT, wild-type

The promyelocytic leukemia (PML) protein is the main structural component of subnuclear domains termed PML nuclear bodies (PML NBs), which are implicated in tumor suppression by regulating apoptosis, cell senescence and DNA repair. Previously, we demonstrated that ATM kinase can regulate changes in PML NB number in response to DNA double-strand breaks (DSBs). PML NBs make extensive contacts with chromatin and ATM mediates DNA damage-dependent changes in chromatin structure in part by the phosphorylation of the KRAB-associated protein 1 (KAP1) at S824. We now demonstrate that in the absence of DNA damage, reduced KAP1 expression results in a constitutive increase in PML NB number in both human U2-OS cells and normal human diploid fibroblasts. This increase in PML NB number correlated with decreased nuclear lamina-associated heterochromatin and a 30% reduction in chromatin density as observed by electron microscopy, which is reminiscent of DNA damaged chromatin. These changes in chromatin ultrastructure also correlated with increased histone H4 acetylation, and treatment with the HDAC inhibitor TSA failed to further increase PML NB number. Although PML NB number could be restored by complementation with wild-type KAP1, both the loss of KAP1 or complementation with phospho-mutants of KAP1 inhibited the early increase in PML NB number and reduced the fold induction of PML NBs by 25–30% in response to etoposide-induced DNA DSBs. Together these data implicate KAP1-dependent changes in chromatin structure as one possible mechanism by which ATM may regulate PML NB number in response to DNA damage.

Introduction

Genomic stability is an important component in preventing the accumulation of mutations in oncogenes and tumor suppressor genes that could lead to cancer.[1,2] The promyelocytic leukemia (PML) protein is a tumor suppressor that has been implicated in DNA repair, cell cycle control and apoptosis,[3-5] processes that act together to maintain genome stability. The PML protein is the major structural component of the subnuclear domain known as the PML nuclear body (PML NB),[3,4] and disruption or loss of these bodies is thought to contribute to tumor progression in both acute promyelocytic leukemia (APL)[6,7] and in several solid tumors including those of the brain, breast, colon, lung and prostate.[8-10] PML-deficient mice, for example, exhibit increased sister-chromatid exchange reminiscent of Bloom's syndrome and have an impaired p53 response to DNA damage.[11-13] In addition, PML deficient mice are particularly susceptible to the formation of tumors in response to carcinogens.[14] Although aberrant apoptosis in PML deficient mice may contribute to their cancer susceptibility, this phenotype could also suggest a broader impairment of DNA damage signaling and repair.

One way that PML NBs may contribute to DNA damage signaling is through the post-translational modification and/or sequestration and release of proteins involved in cell cycle checkpoints, including p53 and Chk2. For example, p53 accumulates at PML NBs following DNA damage and is activated by concomitant phosphorylation and acetylation by HIPK2 and CBP, respectively.[15,16] Chk2 on the other hand, localises to PML NBs prior to DNA damage, leaving the bodies in response to genotoxic stress.[17] Chk2 can also phosphorylate PML at S117 in response to DNA damage and this phosphorylation event plays a role in mediating apoptosis independently of p53.[17] PML in turn is required for the ATM-mediated activation of Chk2 in response to DNA damage by promoting its autophosphorylation.[18] In addition to these checkpoint proteins, a number of other factors involved in DNA damage signaling localise to PML NBs before

*Correspondence to: Graham Dellaire; Email: dellaire@dal.ca
Submitted: 11/16/10; Revised: 12/20/10; Accepted: 12/20/10
DOI: 10.4161/cc.10.2.14551

or after DNA damage including MRE11,[19] TopBP1,[20] and ATR kinase[21] (reviewed in ref. 4). There is also evidence that under certain conditions PML NBs may play a direct role in DNA repair and recombination processes, accumulating ssDNA following UV-irradiation[22] or telomeric DNA in cancer cells that maintain their telomeres by a mechanism known as alternative lengthening of telomeres (ALT).[23] Finally, we and others have reported the close juxtaposition of PML NBs with persistent DNA repair foci 18–24 h after DNA damage by ionizing radiation and chemotherapy agents.[24-27] Therefore, PML NBs may represent important cellular nodes for cell stress signaling and DNA recombination and repair. As such, changes in body number may have a functional impact on the fidelity or efficiency of DNA damage signaling and/or repair, as has been demonstrated for Chk2 and p53 activation by genotoxic stress.[12,13,15-18]

Previously, we and others have demonstrated that diverse forms of DNA damage from UV and chemotherapy agents to ionizing radiation can induce an increase in PML NB number.[20,24-26,28] However, the mechanism for this disruption had not been elucidated nor was it known if this process was regulated. We demonstrated that PML NBs do respond in a dose-dependent fashion to low, physiological levels of DNA damage produced by ionizing radiation and chemotherapy agents that induce DNA double-strand breaks (DSBs), by increasing in number through a fission mechanism from pre-existing bodies.[25] Furthermore, this increase in PML NB number is regulated by NBS1, a component of the MRE11/NBS1/RAD50 (MRN) DNA damage sensor, as well as ATM, ATR and Chk2 kinase,[25] which together constitute parallel and partially redundant signaling pathways for the detection and repair of DNA damage.[29,30] These changes in body number are also concomitant with ultrastructural changes in chromatin that appear to destabilize PML NBs, possibly due to the transmission of topological stress in damaged chromatin to these bodies via extensive chromatin contacts at their periphery.[25,31]

Chromatin organization and epigenetic modification also play an important role in the DNA damage response, controlling access to DNA lesions within chromatin and facilitating the accumulation of the DNA repair machinery (reviewed in ref. 32–34). Changes in chromatin structure following DNA damage occur rapidly and are regulated at least in part by ATM kinase, which may be activated by topological changes in chromatin initiated by the DNA break itself.[35,36] For example, perturbation of chromatin structure by DNA inter-chelating agents such as chloroquine, the inhibition of histone deacetylases (HDACs) and osmotic shock can activate ATM kinase in the absence of DNA damage.[37,38] ATM mediates changes in chromatin structure in response to DNA DSBs in part by phosphorylating chromatin-associated protein KAP1 at S824.[35] KAP1 colocalizes with HP1beta in pericentromeric heterochromatin and is a transcriptional corepressor that regulates the expression of a large number of Krüppel-associated box (KRAB) zinc finger proteins.[39-41] KAP1 has also been implicated in the resolution of persistent DNA repair foci containing the phosphorylated histone H2AX (γ-H2AX), which by virtue of their association with the periphery of pericentric heterochromatin in murine cells at 24 h after treatment with ionizing radiation, are believed to represent unresolved DNA breaks in heterochromatin.[42] In addition, phosho-KAP1 co-localises with γ-H2AX repair foci and 53BP1 as early as 30 min after treatment with ionizing radiation,[43] and phosho-KAP1 remains associated with γ-H2AX in persistent repair foci in conjunction with both active ATM kinase and 53BP1.[44] Taken together, these studies indicate that chromatin changes mediated by the ATM-dependent phosphorylation of KAP1 may facilitate access to damaged DNA within or adjacent to condensed heterochromatin.

Since the activation of ATM by DNA damage results in both changes in chromatin structure via phosphorylation of KAP1, and an increase in PML NB number, we hypothesized that changes in chromatin structure mediated by KAP1 could be responsible, at least in part, for the observed changes in PML NB number elicited by genotoxic stress. We now demonstrate that depletion of KAP1 by RNA interference in both human U2-OS and Tert-immortalized normal human diploid fibroblasts (NHDFs) increases PML NB number, independently of DNA damage and concomitant with epigenetic and structural changes in chromatin that reduce chromatin density within the nucleus. Loss of KAP1 also attenuated the overall increase in PML NB number in response to etoposide-induced DNA DSBs. Finally, we provide evidence that the phosphorylation of KAP1 at S824 by ATM may regulated the initial increase in PML NB number following the induction of DNA DSB by etoposide. Together these data implicate KAP1-dependent changes in chromatin structure as a possible mechanism by which ATM regulates PML NB number following DNA damage.

Results

ATM-dependent KAP1 phosphorylation at S824 peaks during early changes in PML NB number in etoposide-treated NHDFs. Previously, we demonstrated that loss or inhibition of ATM kinase could delay changes in PML NB number in the NHDF cell line GM05757 in response to DNA DSBs induced by etoposide, a DNA topoisomerase II (topo II) inhibitor.[25] One mechanism by which ATM might regulate PML NB number is by modulating changes in chromatin structure in response to DNA DSBs, which in turn destabilizes PML NBs leading to their increase in number by fission from pre-existing bodies. We have recently shown that etoposide-induced DNA damage results in the global decondensation of chromatin,[27] and that ATM can mediate DNA damage-induced changes in chromatin structure via phosphorylation of KAP1 at S824.[35] Therefore, we sought to determine if changes in KAP1 phosphorylation at S824 correlated temporally with changes in PML NB number in response to etoposide-induced DNA DSBs in Tert-immortalized GM05757 NHDFs (5757-TERT) (**Fig. 1**). The pulsed-treatment of these NHDFs with 20 μM etoposide for 0.5 h was sufficient to induce robust activation of ATM kinase as demonstrated by S1981 autophosphorylation and targeted phosphorylation of KAP1 at S824, which was also accompanied by rapid phosphorylation of H2A.X at S139 (**Fig. 1A**). By pulsing etoposide treatment it is possible to produce the equivalent number of DNA DSB breaks

to 2 Gy of ionizing radiation (or ~70–100 breaks) resulting in ~50% clonagenic survival and a well characterized induction of PML NBs in GM05757 NHDFs.[25] ATM activation remained robust until 1 h post-etoposide treatment after which phosphorylation at S1981 was rapidly attenuated between 3 and 6 h recovery from etoposide. H2A.X phosphorylation responded similarly, mirroring the activation of ATM, and returned to basal levels of phosphorylation at 24 h recovery from etoposide. In contrast, KAP1 S824 phosphorylation peaked earlier at 0.5 h during etoposide treatment and began to attenuate as soon as 1 h recovery from etoposide, returning to near basal levels after 3 h recovery. Phosphorylation of KAP1 in response to etoposide-induced DNA DSBs appears to be primarily dependent on ATM kinase in 5757-TERT NHDFs, as the specific inhibition of ATM by the kinase inhibitor KU55933,[45] prevented S824 phosphorylation (**Fig. 1B**). This result is consistent with previous work indicating that the etoposide-induced phosphorylation of KAP1 at S824 is abrogated in ATM-deficient fibroblasts.[46] PML NB number in 5757-TERT cells increased from ~15 to 18 bodies ($p < 0.05$) immediately after 0.5 h of etoposide-treatment and continued to increase to ~21 bodies ($p < 0.01$) from 1 h to 3 h recovery from drug treatment, before returning to near basal levels at 6 h to 24 h (i.e., ~16–17 bodies) post-etoposide treatment (**Fig. 1C and D**), which was similar to the response of the parental GM05757 NHDFs without ectopic TERT expression (**Sup. Fig. 1**). Thus, TERT expression does not affect the PML NB response to DNA damage in this cell line compared to the parental NHDF cell line. Together, these data indicate that KAP1 phosphorylation is an early ATM-dependent event in the DNA damage response to etoposide, and that KAP1 phosphorylation correlates with early changes in PML NB number.

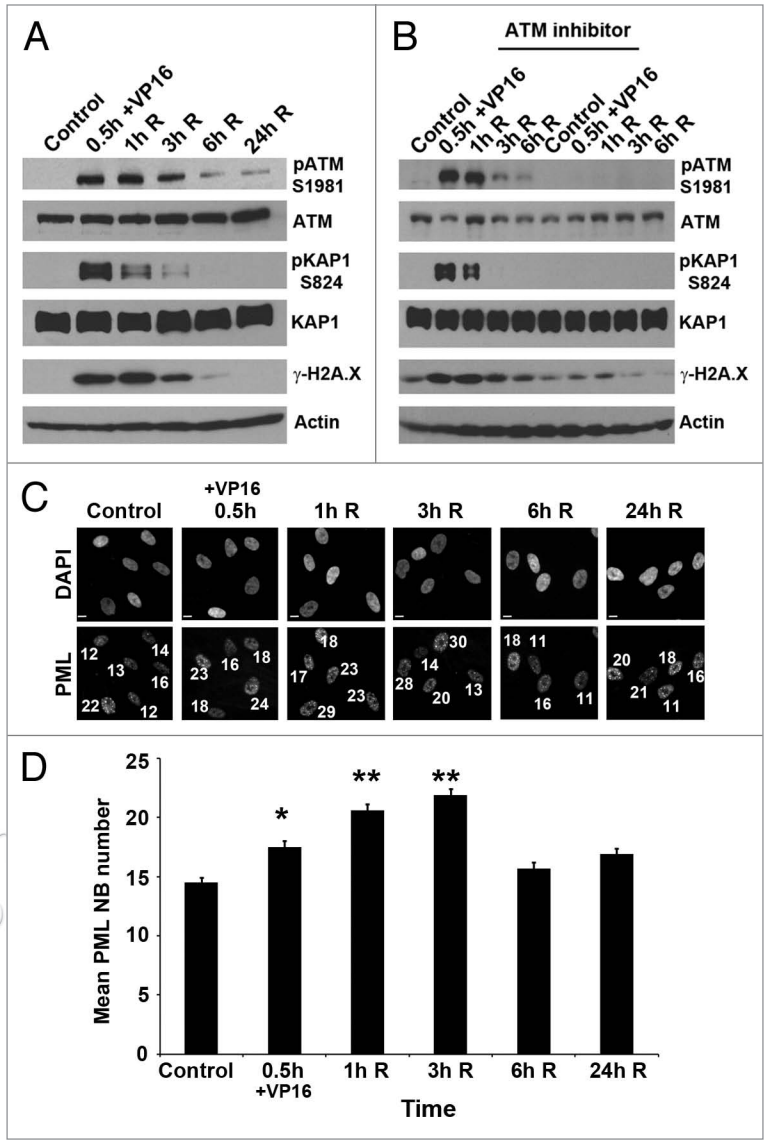

Figure 1. ATM-dependent KAP1 phosphorylation at S824 correlates with early changes in PML NB number. (A) Tert-immortalized NHDFs (5757-TERT) were untreated (Control) or treated with 20 μM etoposide for 0.5 h and left to recover for the indicated time (i.e., 1 h R, 3 h R, 6 h R and 24 h R) before processing for western blotting analysis of γ-H2AX, KAP1 (S824) and ATM (S1981) phosphorylation. Actin and total protein levels of KAP1 and ATM served as loading controls. (B) 5757-TERT were treated as in (A) in growth medium with or without 10 μM ATM inhibitor (KU55933). (C and D), 5757-TERT were treated as in (A) and then processed for the immunofluorescence detection of the PML protein and DNA was counter stained with DAPI. The number of PML NBs per cell is indicated on each panel in (C), and the statistical analysis of PML NB number in 5757-TERT cells treated with etoposide is shown as bar graph in (D). Scale bars = 10 μm and error bars = SEM (n = 90). *$p < 0.05$, **$p < 0.01$.

KAP1 depletion increases PML NB number, independent of cell type and without changes in cell cycle distribution. Although not directly demonstrated at the ultrastructural level, the loss of KAP1 expression appears to alter chromatin organization.[35] We have shown that the integrity and number of PML NBs can be affected by changes in chromatin structure following DNA damage or during DNA replication.[25,47,48] Therefore, we hypothesized that loss of KAP1 might also affect PML NB number in concert with changes in chromatin structure. To test this hypothesis we first analyzed PML NB number in telomerase-deficient human U2-OS osteosarcoma cells stably expressing a short-hairpin RNA (shRNA) directed against either GFP (as a Mock control) or KAP1 (ΔKAP1) (**Fig. 2A**), which had previously been characterized to differ in chromatin structure as determined by micrococcal nuclease sensitivity.[35] The ΔKAP1 U2-OS cells expressing the KAP1 shRNA exhibited a 90% knock-down of KAP1 protein expression and a significant increase in PML NB number compared to the Mock control cells expressing the GFP shRNA (i.e., 13 versus 8 NBs; $p < 0.05$) (**Fig. 2A**). To confirm that this affect was not cell type- or clone-dependent, we generated 5757-TERT NHDF cell lines expressing either the KAP1 (ΔKAP1) or GFP shRNA (Mock) (**Fig. 2B**). In addition, we generated cell lines in which the loss of KAP1 expression in ΔKAP1 cells was complemented by the expression of a wild type KAP1 cDNA (ΔKAP1 + WT KAP1) (**Fig. 2B**) carrying a silent mutation that prevents it from being targeted by the KAP1 shRNA.[35] Depletion of KAP1 in the

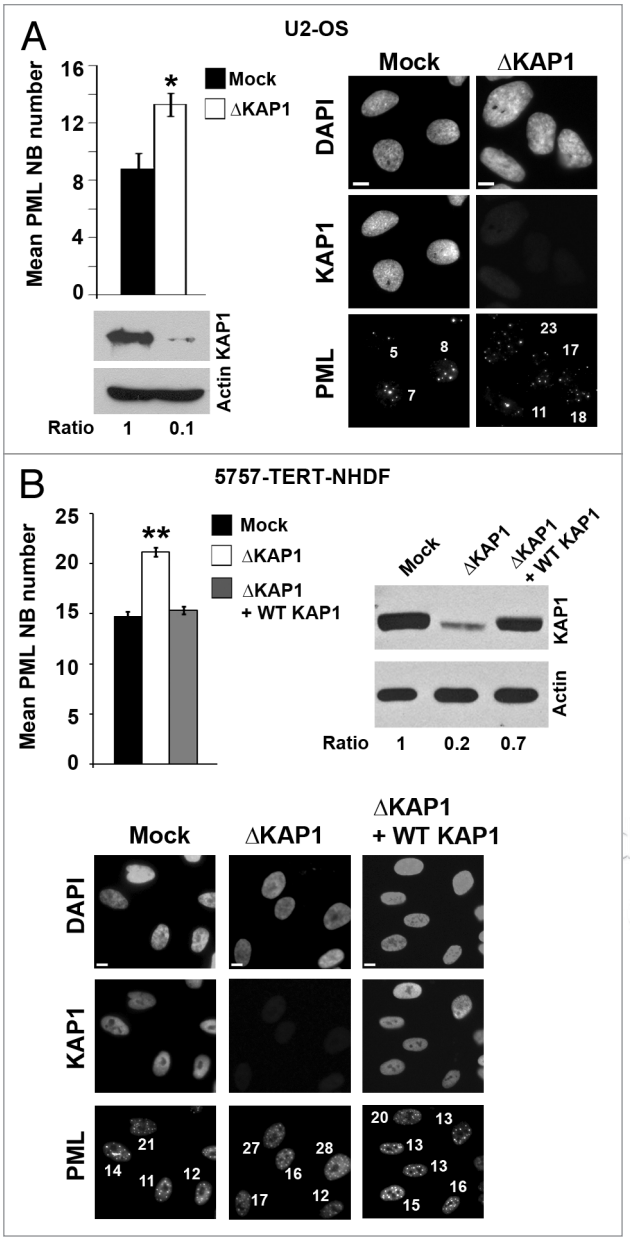

Figure 2. KAP1 depletion induces a constitutive increase in PML NB number in U2-OS and 5757-TERT NHDFs. (A and B), U2-OS (A) or 5757-TERT NHDFs (B) stably expressing either a control unrelated shRNA directed against GFP (Mock) or a shRNA directed against human KAP1 (ΔKAP1) were either fixed and prepared for the immunofluorescence detection of PML (at the right in A or the bottom part in B) or prepared for western blotting analysis using antibodies against KAP1. A bar graph indicates the PML NB number in control (black bar, Mock) and KAP1 depleted (white bar, ΔKAP1) cells. The relative levels of KAP1 protein are shown below the bar graph in (A) and to the right in (B) by western blotting. In addition, PML NB number and KAP1 protein levels were evaluated in ΔKAP1 5757-TERT cells expressing a shRNA resistant wild type KAP1 gene (+WT KAP1) are shown in the bar graph (grey bar) and western blot in (B). Actin was used as a loading control for western blot analysis and the level of KAP1 was determined by densitometry relative to actin (Ratio). The number of PML NBs per cell is indicated on each cell shown in (A and B), and DNA was counterstained with DAPI. Scale bars = 10 μm and error bars = SEM (n = 90). *p < 0.05, **p < 0.001.

5757-TERT NHDFs by ~80% caused a concomitant increase in PML NB number from ~15 to 21 NBs ($p < 0.001$). This effect on PML NB number was confirmed to be dependent on KAP1 protein levels and not off-site targeting of other RNAs by the KAP1 shRNA, as restoration of KAP1 protein levels by wild type KAP1 in these cells caused a reduction in PML NB number to control levels (~15 NBs) (**Fig. 2B**). Since we observed an increase in PML NB number in response to KAP1 depletion in both 5757-TERT NHDFs and U2-OS cells, which do not express TERT and maintain their telomeres by the alternative lengthening of telomeres (ALT) pathway,[49] it is also unlikely that TERT expression is responsible for the observed affects of KAP1-depletion on PML NB number.

One possible explanation for the observed effects of KAP1 depletion on PML NB number is that loss of KAP1 may alter the cell cycle distribution of the 5757-TERT cells. We and others have demonstrated that PML NB number is altered through the cell cycle and can double in number as cells progress from G_1- to G_2-phase.[47,50,51] In particularly, PML NB number can dramatically increase during S-phase.[47] As such, a significant accumulation of cells in S- or G_2-phase, and a reduction of cells in G_1, would result in an increase in the average PML NB number. Therefore, we examined the cell cycle distribution of asynchronously dividing GFP shRNA (Mock) and KAP1 shRNA expressing 5757-TERT NHDFs (ΔKAP1) (**Fig. 3**). We found that depletion of KAP1 had little effect on the cell cycle distribution of these cells, consistent with our previous studies of KAP1 depletion in U2-OS human osteosarcoma cells.[35] We also observed a similar cell cycle distribution on average between biological replicates and in ΔKAP1 cells complemented with WT KAP1 (**Sup. Fig. 2**). Together these data indicated that the induction of PML NBs by the depletion of KAP1 was cell type independent and did not arise because of a change in the cell cycle profile of ΔKAP1 cells.

Characterization of ultrastructural changes in chromatin induced by KAP1 depletion. KAP1 depletion in U2-OS cells can induce an increase in the micrococcal nuclease (MNase) sensitivity of chromatin, suggesting a global change in chromatin organization,[35] and PML NBs are responsive to changes in chromatin organization.[25,47,48] Therefore, gross changes in chromatin structure induced by KAP1 depletion could partially explain the observed increase in PML NB in ΔKAP1 U2-OS and Tert-immortalized NHDFs cells. However, to date the effects of KAP1 depletion on interphase chromatin structure have only been inferred from MNase digestion and remain to be confirmed by high resolution techniques that can visualize chromatin in situ within cells, such as electron microscopy. To more directly determine the impact of KAP1 depletion on chromatin organization we examined chromatin organization within the nuclei of control (Mock) or KAP1 depleted 5757-TERT NHDFs (ΔKAP1) by electron spectroscopic imaging (ESI) (**Figs. 4 and 5**).

ESI allows the unequivocal identification of chromatin within the nucleus at high resolution by directly observing the elemental signature of cellular components including nucleic acids and proteins.[52] For example, electron micrographs of nitrogen can be used to determine the location of nucleic acids and proteins within the cell, and phosphorus can be used to image nucleic acids. In

addition, the nitrogen and phosphorus electron micrographs can be subtracted from each other allowing the segmentation of chromatin (in yellow) from non-chromosomal protein complexes (in blue) (**Fig. 4**). KAP1 colocalises with heterochromatin protein 1 (HP1) isoforms[39,53] and can recruit the methyltransferase SETDB1 to mark heterochromatin domains epigenetically via tri-methylation of histone H3 lysine 9 (H3-MeK9), which in turn can recruit HP1.[54] Unlike murine cells which exhibit large arrays of pericentric heterochromatin within chromocenters, heterochromatin within human fibroblast cells is more widely distributed.[55] Nonetheless, concentrations of higher-order chromatin fibers consistent with heterochromatin can be identified by ESI in association with the nucleolus, centromeres and the nuclear lamina.[52]

Using ESI, we observed that the thickness of blocks of heterochromatin associated with the nuclear lamina appeared to be greater in control (Mock) (**Fig. 4A**) than in ΔKAP1 5757-TERT NHDFs (**Fig. 4B**). Depletion of KAP1 reduced the overall thickness of the dense chromatin associated with the nuclear lamina from 260 ± 20 nm in WT cells to 120 ± 10 nm in ΔKAP1 cells ($p < 0.001$) (**Fig. 4C**), which is consistent with the decondensation of heterochromatin associated with the nuclear lamina in ΔKAP1 cells. In addition, by segmenting chromatin from other nuclear components in the ESI micrographs it is possible to determine changes in density or packing of chromatin fibers.[27] Using this procedure, we analyzed the global density of chromatin throughout the nucleus of Mock and ΔKAP1 5757-TERT NHDFs (**Fig. 5**). In ΔKAP1 cells, chromatin appeared to occupy a reduced percentage of the total area of the nucleus in our ESI micrographs (**Fig. 5A**), which could be quantified as a ~30% reduction in chromatin density from 24 ± 1% to 17 ± 1% of the total nuclear volume ($p < 0.001$) (**Fig. 5B**). This reduction in chromatin density also correlated with increased MNase sensitivity of chromatin isolated from ΔKAP1 versus Mock NHDFs, which is again consistent with the decondensation of chromatin in ΔKAP1 cells (**Sup. Fig. 3**). These data provide the first ultrastructural characterization of changes in chromatin structure in situ after KAP1 depletion, and indicate that loss of KAP1 results in reduced chromatin density and altered heterochromatin organization in human fibroblast nuclei.

Increased histone acetylation correlates with elevated PML NB number. In both yeast and mammals, histone acetylation plays an important role in DNA repair (reviewed in ref. 32–34). For example, histone H4 is targeted for acetylation by the TIP60 acetylase complex in chromatin within the vicinity of a DNA break[56] and loss of TIP60's acetylase activity is associated with impaired DNA DSB repair and apoptosis.[57] In addition, prolonged treatment of cells with high concentrations of HDAC inhibitors can activate ATM kinase in the absence of DNA damage, suggesting that the decondensation of chromatin induced by histone acetylation may facilitate both activation of DNA damage signaling as well as access to DNA lesions.[58] To determine the relationship between histone acetylation and PML NB number we treated GFP shRNA (Mock) and KAP1 shRNA expressing 5757-TERT NHDFs (ΔKAP1) with the HDAC inhibitor TSA (**Fig. 6**). We chose to use 200 ng/ml of TSA in our experiments as this was above the concentration shown to induce chromatin decondensation in 4 h (i.e., 100 ng/ml)[59] and well below the concentration previously shown to activate ATM kinase (i.e., 10 μM).[38] Under these conditions, we were able to see a robust increase in histone H4 acetylation (~10–11 fold) within 4 h to 6 h in the Mock cells without inducing ATM kinase activation as indicated by western blot analysis of ATM phosphorylation at S1981 (**Fig. 6A**). We also found that ΔKAP1 cells exhibited ~5-fold increase in basal histone H4-acetylation compared to Mock cells prior to TSA treatment and that HDAC inhibition in these cells only marginally increased H4 acetylation (**Fig. 6A**). TSA treatment for 4 h was sufficient to cause a dramatic increase in PML NB number in Mock cells expressing normal levels of KAP1, increasing from ~16 to 22 bodies ($p < 0.001$), but had little effect on the number of PML NBs in ΔKAP1 cells (**Fig. 6A and B**). Although there appeared to be enhanced ATM protein expression in the TSA treated ΔKAP1 cells, we found similar levels of ATM between Mock and ΔKAP1 NHDFs in the absence of TSA treatment (**Sup. Fig. 4**), which is also consistent with our previous analysis of ATM protein levels in Mock and KAP1-depleted U2-OS cells.[35] Together with our ultrastructural studies of chromatin in KAP1-depleted NHDFs, these data indicate that the epigenetic and structural changes in

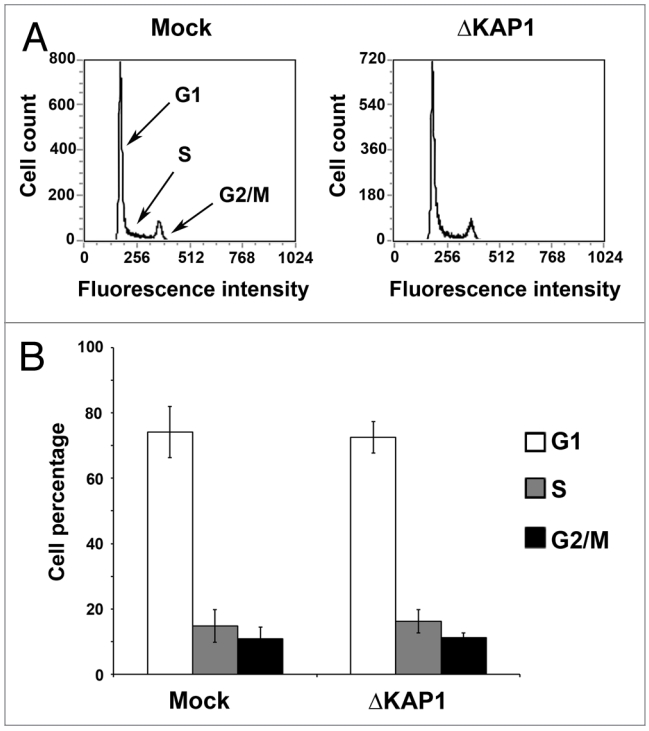

Figure 3. KAP1 depletion does not significantly alter the cell cycle profile of 5757-TERT NHDFs. (A) Asynchronously growing, 5757-TERT NHDFs stably expressing either a control unrelated shRNA directed against GFP (Mock) or a shRNA directed against human KAP1 (ΔKAP1) were fixed and prepared for FACs analysis to determine their cell cycle profile. The fluorescence intensity plots are shown for both Mock (right) and ΔKAP1 (left) cells. (B) A bar graph of the relative percentage of cells in G_1, S and G_2/M phase of the cell cycle is also shown for Mock (black bars) and ΔKAP1 (white bars) cells. Error bars = SD (n = 3).

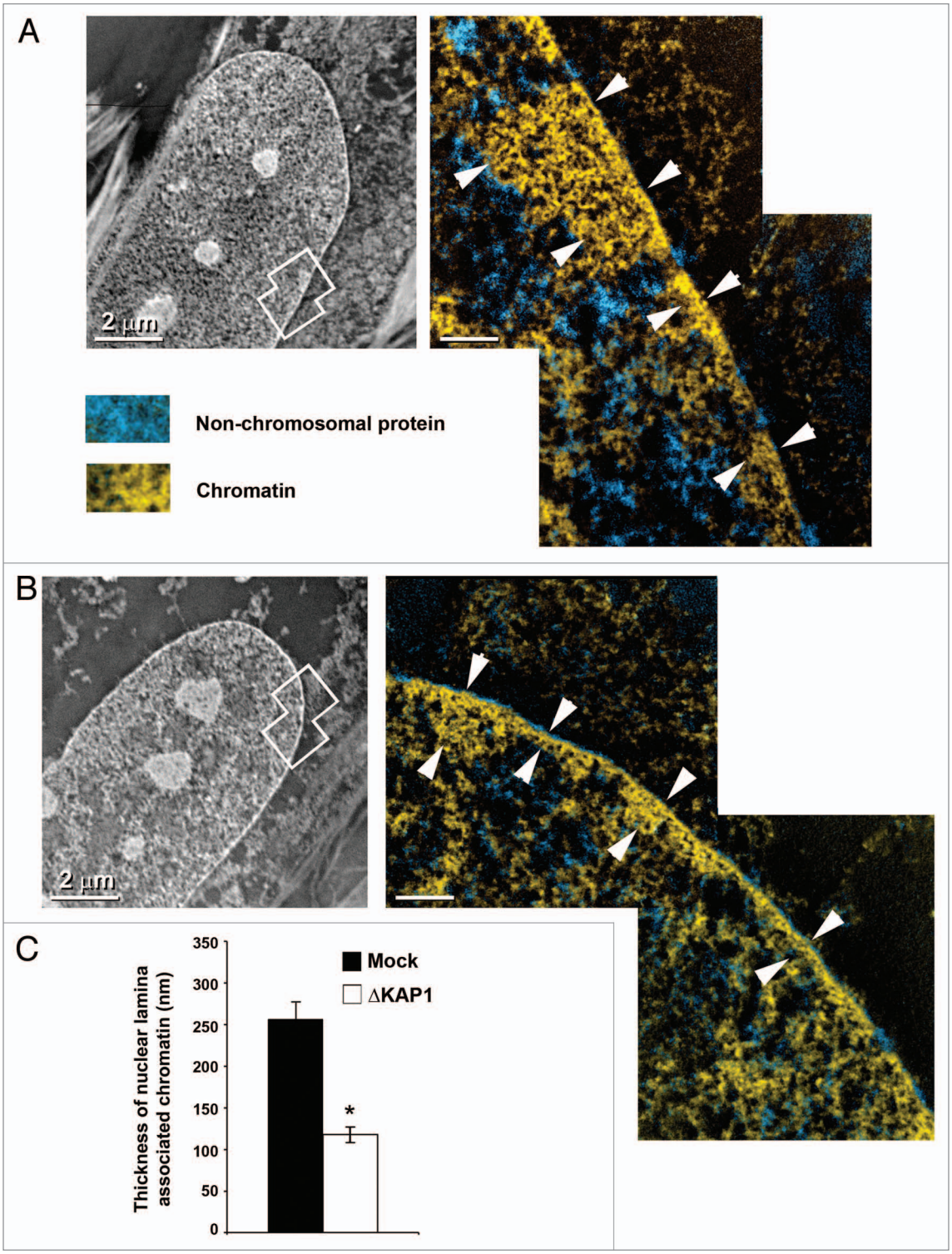

Figure 4. Characterization of changes in nuclear lamina-associated chromatin in KAP1 depleted 5757-TERT NHDFs. (A and B) Control (Mock, A) or 5757-TERT NHDFs stably expressing a shRNA directed against human KAP1 (ΔKAP1, B) were fixed and prepared for electron spectroscopic imaging (ESI). In each part, a low magnification phosphorus enriched (155 KeV) ESI micrograph is shown of the same cells imaged at higher magnification at the left. The overlapping white rectangles indicate an area of the cell imaged at higher magnification at the right, where chromatin (yellow) and non-chromosomal protein (cyan) have been segregated and false-colored in a composite electron micrograph. Nuclear-lamina associated chromatin, consistent with condensed heterochromatin is indicated between the white arrows. (C) The mean thickness of the condensed chromatin associated with the nuclear lamina was evaluated between Mock (black bars) and ΔKAP1 (white bars) cells and depicted as a bar graph. Scale bars = 200 nm, unless otherwise indicated. Error bars = SEM (n = 50). *p < 0.001.

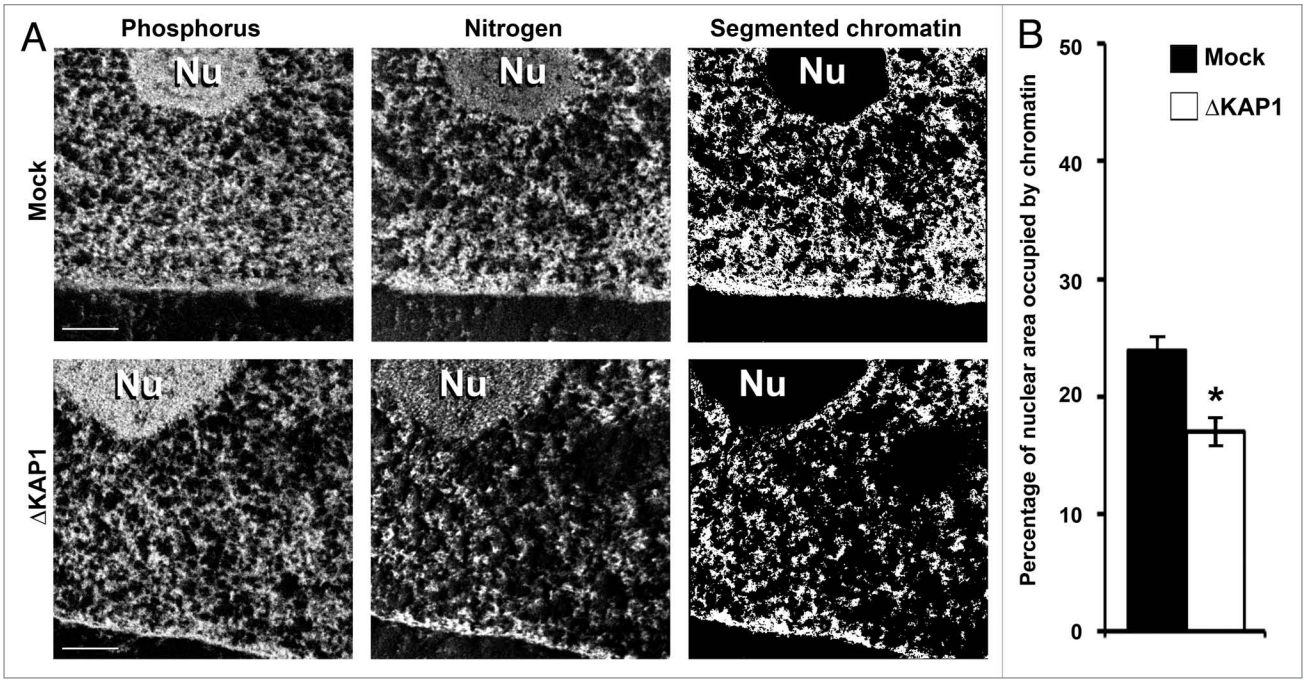

Figure 5. Chromatin density is reduced by KAP1 depletion in 5757-TERT NHDFs. (A) Control (Mock) or 5757-TERT NHDFs stably expressing a shRNA directed against human KAP1 (ΔKAP1) were fixed and prepared for electron spectroscopic imaging (ESI). Separate phosphorus and nitrogen ESI micrographs are shown at the left and a binary mask of segmented chromatin is shown at the far right. (B) A bar graph is shown depicting the analysis of chromatin density within Mock (black bar) or ΔKAP1 (white bar) cells. Scale bars = 500 nm and error bars = SEM (n = 50). *p < 0.001.

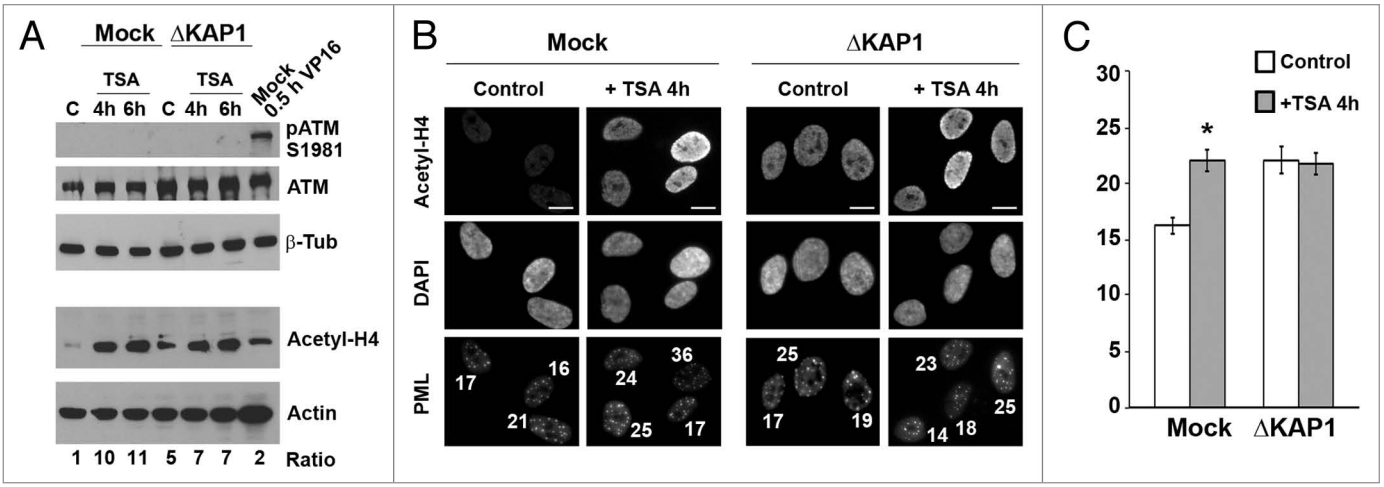

Figure 6. Increased histone acetylation correlates with elevated PML NB number in KAP1 depleted 5757-TERT NHDFs. (A) 5757-TERT NHDFs stably expressing a control unrelated shRNA directed against GFP (Mock) or a shRNA directed against human KAP1 (ΔKAP1), where treated with vehicle (Control) (0.1% DMSO) or with 200 ng/ml of the HDAC inhibitor trichostatin A (TSA) for 4 h or 6 h prior to western blot analysis of ATM, phosphorylated ATM (pATM S1981), and acetylated histone H4 (Acetyl-H4). Actin and beta-tubulin (β-Tub) where used as loading controls and the ratio of acetylated histone H4 protein levels to actin are indicated. (B and C) Mock or ΔKAP1 5757-TERT NHDFs were treated as above with (+TSA) or without (Control) TSA for 4 h before processing for the immunofluorescence analysis of PML and histone H4 acetylation (Acetyl-H4). The number of PML NBs is indicated in the fluorescence micrograph in (B) and represented as a bar graph in (C). To Scale bars = 10 μm and error bars = SEM (n = 60). *p < 0.001.

chromatin mediated by the loss of KAP1 are likely contributors to the observed increase in PML NB number seen in ΔKAP1 cells.

Early DNA damage-dependent changes in PML NB number are inhibited by loss of KAP1 and the expression of S824 phospho-mutants of KAP1. To examine the effect that the loss of KAP1 might have on the induction of PML NB number by DNA DSBs, control 5757-TERT NHDFs cells expressing a GFP shRNA (Mock), KAP1 depleted (ΔKAP1) and KAP1-depleted NHDFs reconstituted with human KAP1 (ΔKAP1 + WT KAP1) were treated with etoposide (**Fig. 7A–C and Sup. Fig. 5**). Averaging the response of two biological replicates of

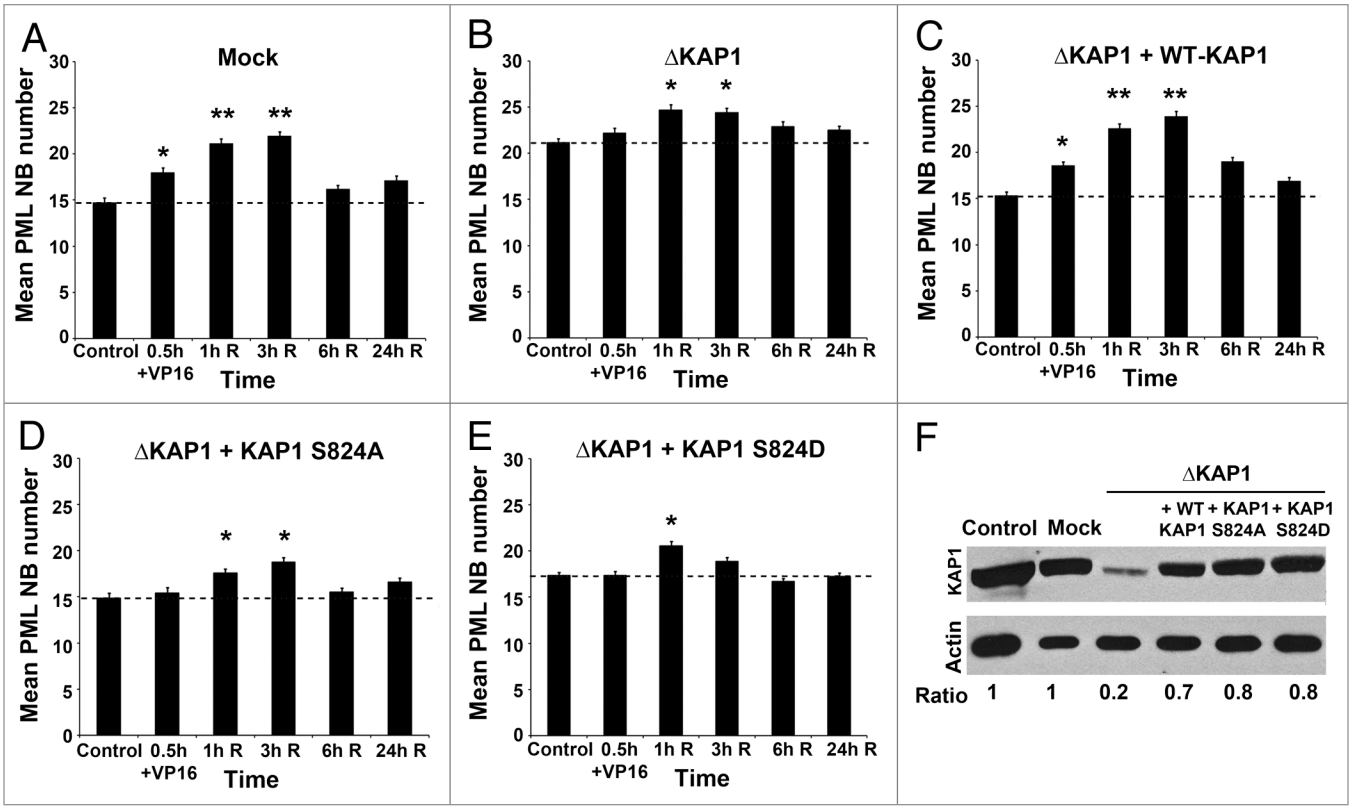

Figure 7. Characterization of the effect of KAP1-depletion or the expression of KAP1 phospho-mutants on PML NB number in response to etoposide in 5757-TERT NHDFs. (A–E) 5757-TERT NHDFs stably expressing a control unrelated shRNA directed against GFP (Mock), a shRNA directed against human KAP1 (ΔKAP1) and ΔKAP1 5757-TERT cells expressing either a wild type KAP1 (ΔKAP1 + WT-KAP1), or two different phospho-mutants of KAP1 (+KAP1 S824A or +KAP1 S824D) were left untreated (Control) or treated with 20 μM etoposide for 0.5 h before recovery for the indicated time (i.e., 1 h R, 3 h R, 6 h R and 24 h R) before processing for the immunofluorescence detection of PML and the counting of PML NBs. A comparison of the mean PML NB number for each cell line in response to etoposide over time is depicted as bar graph for Mock (A), ΔKAP1 (B), ΔKAP1 + WT-KAP1 (C), ΔKAP1 + KAP1 S824A (D) and ΔKAP1 + KAP1 S824D cells (E). (F) Western blot analysis of KAP1 protein levels in representative Mock, ΔKAP1, ΔKAP1 + WT-KAP1, ΔKAP1 + KAP1 S824A, and ΔKAP1 + KAP1 S824 5757-TERT NHDFs. Actin was used as a loading control for western blot analysis and the level of KAP1 was determined by densitometry relative to actin (Ratio). Two biological replicates of each cell line were analyzed for PML NB number in triplicate. The dotted line across each bar graph indicates the initial number of PML NBs prior to etoposide treatment. Error bars = SEM between n = 6 replicates. *$p < 0.05$, **$p < 0.01$.

each cell line, etoposide-treatment induced a similar and significant increase in PML NB number in Mock (**Fig. 7A**) and ΔKAP1 + WT KAP1 cells (**Fig. 7C**) after both 0.5 h of drug treatment (i.e., from ~15 to 18 or 19 NBs, respectively ($p < 0.05$)) and after 1 h recovery from etoposide (i.e., from ~15 to 21 or 23 NBs, respectively ($p < 0.01$)) compared to untreated cells. Whereas, the ΔKAP1 cells did not show a significant increase in PML NB number until at least 1 h to 3 h post-etoposide treatment, where body number increased to 25 from 21 NBs in untreated cells ($p < 0.05$) (**Fig. 7B**). PML NB number peaked in both Mock and WT KAP1 expressing 5757-TERT NHDFs at 3 h post-etoposide treatment at ~22 and 24 NBs (respectively) before declining to ~17 NBs by 24 h after drug treatment (**Fig. 7A and C**). PML NB number in ΔKAP1 cells also declined from 6 to 24 h post-etoposide treatment but remained well above the level of NBs seen in cells expressing WT KAP1 (**Fig. 7B**). In addition, the fold increase in PML NB number at 3 h recovery from etoposide was reduced by 25–30% in ΔKAP1 cells compared to either Mock cells or NHDFs expressing WT KAP1 (1.15 versus either 1.49 or 1.56, respectively) (**Table 1**). Thus, loss of KAP1 expression elevated the basal level of PML NBs in these cells and generally inhibited the further induction of PML NB number in response to etoposide-induced DNA DSBs.

Loss of ATM expression can inhibit changes in PML NB number in response to etoposide-induced DNA DSBs,[25] and KAP1 phosphorylation by ATM mediates DNA DSB-induced chromatin decondensation,[35] which might provide a mechanism for changes in PML NB number. We observed early and rapid changes in KAP1 phosphorylation at S824 in response to etoposide in 5757-TERT NHDFs (**Fig. 1A**), peak phosphorylation of KAP1 coincided with the initial DNA DSB-dependent increase in PML NB seen after 0.5 h of drug treatment (**Fig. 1C and D**), and this increase can be abrogated by loss of KAP1 expression (**Fig. 7A and B**). Thus, ATM may regulate PML NB number in response to DNA damage, in part, via KAP1 phosphorylation. To test this possibility, we generated ΔKAP1 5757-TERT cells lines reconstituted with phospho-null (S824A) or phospho-mimetic

(S824D) mutants of human KAP1, and determined the PML NB response to etoposide-induced DNA DSBs in these cells (**Fig. 7D and E and Sup. Fig. 6**). Although KAP1 depleted NHDFs stably expressing the KAP1 S824A phospho-null mutant cDNA had a similar number of PML NBs prior to etoposide-treatment as the WT KAP1 or Mock control cells (**Fig. 7D**), 5757-TERT NHDFs expressing the S824D phospho-mimetic mutant cDNA exhibited a significantly increased number of PML NBs compared to control cells (i.e., from ~15 to 17 PML NBs; $p < 0.05$) (**Fig. 7E**). Cell cycle profile analysis of KAP1 S824D expressing ΔKAP1 5757-TERT NHDFs, indicated an increase in G_2 (from ~10 to 15%) and a reduced accumulation of these cells in S-phase (from ~14 to 10%), as compared to Mock, WT and KAP1 S824A expressing NHDFs (**Sup. Fig. 2**). However, the increased percentage of cells in G_2-phase of the cell cycle was not significant ($p = 0.25$) when averaged between two biological replicates. After 0.5 h of etoposide treatment, unlike control cells or NHDFs expressing WT KAP1 (**Fig. 7C**), PML NB number in NHDFs expressing both KAP1 phospho-mutants failed to increase significantly, indicating that disruption of normal KAP1 phosphorylation can inhibit early etoposide-induced changes in PML NB number (**Fig. 7D and E**). These observed changes were not a result of differences in the expression of WT or KAP1 mutant cDNAs as we chose cells lines with nearly equivalent expression levels of KAP1 (**Fig. 7F**). PML protein levels and isoform expression were also very similar between Mock and ΔKAP1 NHDFs, with and without complementation with WT KAP1 or the phospho-mutants (**Sup. Fig. 7**). In addition, because the banding pattern seen for the PML protein by western blot analysis represents not only PML protein splice-isoforms but also the abundance of sumoylated isoforms of PML (**Sup. Fig. 7**),[60] we conclude that sumoylation of PML and its isoforms is also similar between these cell lines.

Cells expressing both KAP1 phospho-mutants demonstrated a significant increase in PML NB number at 1 h post-etoposide treatment (e.g., increasing from 15 to 18 NBs in KAP1 S824A cells; $p < 0.05$) (**Fig. 7D and E**). However, body number peaked earlier at 1 h recovery from etoposide in KAP1 S824D cells (i.e., increasing from 17 to 21 NBs; $p < 0.05$) (**Fig. 7E**) compared to controls cells (Mock) or cells expressing either WT or S824A KAP1, which peaked at 3 h recovery from etoposide (**Fig. 7C and D**). In addition, the fold increase in peak PML NB number after etoposide-treatment compared to untreated cells was again reduced by 25–30% for cells expressing both the S824D and S824A KAP1 phospho-mutants (i.e., a 1.18 and 1.26 fold increase at 1 h and 3 h recovery, respectively) compared to 5757-TERT cells expressing WT KAP1 (i.e., a 1.56 fold increase at 3 h recovery) (**Fig. 7C and E**) (**Table 1**). Together these data implicate phosphorylation of KAP1 at S824 in the early induction of PML NB number in response to etoposide induced DNA DSBs.

Table 1. Fold change in PML NB number over time in response to etoposide

			Recovery			
Cell line	**Control**	**0.5 h VP16†**	**1 h**	**3 h**	**6 h**	**24 h**
Mock	1	*1.22	1.43	1.49	1.10	1.16
ΔKAP1	1	1.05	1.17	1.15	1.08	1.06
+ WT KAP1	1	1.21	1.47	1.56	1.24	1.10
+ KAP1 S824A	1	1.05	1.20	1.26	1.06	1.13
+ KAP1 S824D	1	1.00	1.18	1.09	0.96	0.99

*Fold change was derived from the mean change in PML NB number between two biological replicates. †Cells were treated for 0.5 h with 20 μM etoposide (VP16) and left to recovery for the indicated times.

Discussion

Many forms of genotoxic stress can increase PML NB number and alter their biochemical composition, suggesting these characteristic changes in PML NBs are likely a universal response to DNA damage.[3,4] We previously demonstrated that the induction of PML NBs is regulated by ATM kinase and hypothesized that both changes in chromatin structure induced by DNA damage, and/or signaling events initiated by ATM, were responsible for the observed change in PML NB number in response to DNA DSBs.[25] However, the mechanistic details of how ATM mediates changes in PML NB number were not elucidated. In this study, we used the well characterized response of PML NBs in NHDF cells treated with the topo II inhibitor etoposide to address the mechanism by which ATM regulates PML NB number in response to DNA DSBs. Our study provides the first evidence of a possible mechanism by which ATM regulates PML NB number via KAP1-mediated changes in chromatin organization. Below we discuss these results in the context of the cellular DNA damage response and the possible role that changes in PML NB number may play in DNA damage signaling and repair.

KAP1-depletion results in changes in chromatin organization reminiscent of those seen following DNA damage. Previously, we demonstrated that depletion of KAP1 could alter the MNase sensitivity of chromatin and that KAP1 phosphorylation at S824 was responsible for increased nuclease sensitivity of chromatin following the induction of DNA DSBs by neocarzinostatin.[35] In addition, the peak sensitivity of chromatin to MNase after DNA damage correlated with the peak phosphorylation of KAP1 at S824.[35] In our current study, depletion of KAP1 resulted in a constitutive increase in PML NB number as well as changes in chromatin organization as observed by electron microscopy. These changes included a reduction in nuclear lamina-associated heterochromatin (**Fig. 4**), consistent with decondensation of heterochromatin at the nuclear envelope, and a 30% reduction in the area of nucleus occupied by chromatin in our electron micrographs (**Fig. 5**). We interpret this decrease in area occupied by chromatin as a reduction in the density of chromatin fibers within the nucleus. Chromatin density changes can occur when 10 or 30 nm fibers of chromatin become more (or less) closely packed together as well as during changes in chromatin condensation state, for example as 30 nm or higher order chromatin fibers decondense into 10 nm chromatin fibers.[61] Therefore, one should not rely on chromatin density measurements alone as an indication of changes in the condensation state of chromatin, and for this reason we also chose to observe changes in the thickness of higher order chromatin fibers associated with the nuclear envelope (**Fig. 4**). Taken together, these

data indicate that KAP1 depletion affects the condensation state of heterochromatin, as well as more generally affecting chromatin density throughout the nucleus.

We and our colleagues have demonstrated that reduced chromatin density also correlates positively with the decondensation of higher order chromatin fibers within tracts of UV-laser induced DNA damage.[36] In addition, the chromatin density changes seen in ΔKAP1 5757-TERT NHDFs are reminiscent of etoposide-induced changes in chromatin structure, where we also characterized a 30% reduction in chromatin density by electron microscopy.[27] However, the observed changes in chromatin density in ΔKAP1 cells did not coincide with the appearance of non-chromosomal protein accumulations (**Fig. 4**), which is in contrast to etoposide treated NHDFs.[27] These non-chromosomal protein accumulations contain the MRN complex and presumably other DNA repair factors that have been recruited into repair foci associated with DNA DSBs.[27] As a corollary to these observations, changes in chromatin density induced by KAP1-depletion may be insufficient to initiate ectopic DNA damage signaling; and consistent with this hypothesis, we did not observe an increased appearance of repair foci in ΔKAP1 5757-TERT NHDFs compared to control cells in the absence of DNA damage (data not shown). Similarly, although changes in chromatin organization induced by chloroquine and osmotic shock can activate ATM kinase, no γ-H2AX repair foci were observed in treated cells.[38] Finally, we observed a five-fold increase in histone H4-acetylation in ΔKAP1 versus Mock NHDFs (**Fig. 6**). Although increased histone acetylation has been shown for specific gene promoters in KAP1 knock-out mice and in the reactivation of endogenous retroviruses in KAP1 null murine embryonic stem cells,[62,63] this is the first demonstration of the global hyperacetylation of histone H4 as a result of KAP1-depletion. Histone H4-acetylation mediated by the TIP60 complex is also associated with DNA damaged chromatin and may facilitate access of repair machinery to DNA lesions.[56,58] Thus, although KAP1 depletion most likely increases histone acetylation indirectly, the directed acetylation of chromatin at DNA breaks is likely to contribute to structural changes in chromatin that would affect PML NB number following DNA damage. Furthermore, treatment with the HDAC inhibitor TSA failed to further increase PML NB number and only slightly increased histone H4-acetylation in ΔKAP1 NHDFs; whereas similar treatment of Mock NHDFs dramatically increased both PML NB number and histone H4-acetylation (**Fig. 6**). In sum, these data both confirm that the MNase sensitivity seen in KAP1-depleted cells does indeed result from changes in chromatin organization, and indicate that the increase in PML NB number in ΔKAP1 5757-TERT cells most likely occurs as a result of structural and epigenetic changes in chromatin rather than inappropriate DNA damage signaling.

KAP1-mediated changes in chromatin structure provide a possible mechanism by which ATM may regulate the early induction of PML NB number. Inhibition or loss of ATM kinase results in an impairment in the early induction of PML NB number in response to both etoposide and ionizing radiation.[25,26] These data point to a general role for ATM in regulating the response of PML NBs to DNA DSBs but do not address the possible mechanisms responsible for ATM-dependent PML NB induction. PML NBs make extensive contacts with the surrounding chromatin[31] and are destabilized by changes to chromatin structure mediated by entry into S-phase, transcriptional inhibition and apoptosis.[47,48] DNA damage itself can initiate the rapid decondensation of chromatin,[36] and in response to DNA DSBs, this process is mediated, at least in part, by the phosphorylation of KAP1 at S824 by ATM.[35] Previously, we have shown that DNA DSBs produced by doxorubicin, etoposide and ionizing radiation cause similar and dose-dependent changes in PML NB number in NHDFs.[25] In the present study, we chose to use etoposide to generate DNA DSBs because of the well characterized changes in chromatin ultrastructure and PML NB number induced by this drug in the NHDF cell line GM05757, which was used to derive the Tert-immortalized cell line in this study.[25,27] We found that in Tert-immortalized NHDFs (5757-TERT), KAP1 is rapidly phosphorylated at S824 in an ATM-dependent manner within 30 min following the induction of DNA DSBs by etoposide (**Fig. 1A and B**), which coincided with the previously characterized increase in PML NB number in response to this drug (**Fig. 1C and D**).[25] These data led us to hypothesize that ATM via KAP1 might provide a likely mechanism for ATM-dependent changes in PML NB number in response to etoposide. Indeed, when KAP1 levels were depleted by RNA interference in both human U2-OS osteosarcoma cells and 5757-TERT NHDFs, PML NB number increased significantly in a cell type-independent manner, and in the absence of DNA damage (**Fig. 2**). In addition, both control (Mock) and KAP1-depleted (ΔKAP1) U2-OS cells[35] and 5757-TERT NHDFs (**Fig. 3**) showed similar cell cycle profiles, suggesting that the observed increase in PML NB number did not arise due to changes in the cell cycle distribution of ΔKAP1 cells. We also found that PML protein isoform expression was also similar between Mock and ΔKAP1 5757-TERT NHDFs (**Sup. Fig. 7**), indicating that the observed changes in PML NB number did not arise due to alterations in PML isoform expression or sumoylation. Complementation of ΔKAP1 5757-TERT NHDFs with wild type KAP1 (**Fig. 2B**) or a non-phosphorylaTable S824A mutant of KAP1 (**Fig. 7B**), resulted in PML NB number returning to that seen in NHDFs prior to KAP1 depletion. However, complementation of ΔKAP1 NHDFs with the phospho-mimetic S824D mutant of KAP1 resulted in only a partial reduction in PML NB number, remaining significantly higher in these cells than in control NHDFs with normal levels of KAP1 (**Fig. 7B**). The cell cycle profile of KAP1 S824D expressing ΔKAP1 NHDFs did show differences in the percentage of cells in G_2 and S phase but these differences were not significant when averaged between biological replicates. Even so, the magnitude of these cell cycle profile changes would not be anticipated to significantly alter PML NB number as the percentage of cells in G_1 was relatively the same between cell lines (~75% on average) and the reduced percentage of cells in S-phase in these cells (**Sup. Fig. 2**) would actually slightly reduce overall body number, as 5757 NHDFs exhibit the greatest increase in PML NB number during S-phase.[25] Nonetheless, the modest increase in body number we observed in KAP1 S824D compared to Mock or WT KAP1 expressing cells (i.e., from 15 to 17 bodies)

(**Fig. 7**) does indicate that KAP1 phosphorylation at S824 can contribute to changes in PML NB number. Furthermore, loss of KAP1 or expression of either phospho-mutant of KAP1 inhibited the early increase in PML NB number after 30 min etoposide and generally reduced the overall induction of PML NBs at later time points by 25–30% (**Fig. 7A and B**). Since KAP1 phosphorylation at S824 peaks after 30 min etoposide treatment and only persists for 1 h after recovery from the drug (**Fig. 1A**), these data are consistent with ATM mediating primarily the early induction of PML NB number in response to DNA breaks via KAP1 phosphorylation. In contrast, after 24 h recovery from etoposide, PML NB number was similar among control cells and ΔKAP1 NHDFs expressing either phospho-mutant of KAP1 (**Fig. 1B**). Thus, KAP1 does not appear to play a role in regulating PML NB number at these later time points. Although we cannot exclude a role for the phosphorylation of other factors by ATM such as Chk2 or even PML itself in the regulation of PML NB biochemical composition or integrity following DNA damage, these data do provide the first evidence for KAP1 as a downstream mediator by which ATM can regulate PML NB number.

PML NBs and the DNA damage response: Why does body number matter? The PML protein and PML NBs are implicated in a host of cellular functions including gene regulation, cell senescence, apoptosis and DNA damage signaling and repair, all of which contribute to tumor suppression.[3,4] Several models of PML NB function have been developed to try to reconcile how one subnuclear domain can be involved in so many diverse cellular functions. Initially, PML NB were thought to solely function as storage sites for nuclear proteins, allowing the cell to maintain appropriate levels of various proteins within the nucleoplasm.[64] As the list of PML NB-associated proteins began to grow and their functions characterized, it was clear that these bodies might also play roles in regulating gene expression by sequestration and release of transcriptional repressors (e.g., Daxx),[65,66] and activators (e.g., CBP).[67] Many of the PML NB-associated proteins are also involved in the post-translational modification of other proteins, including transcription factors like p53, which is modified by phosphorylation and acetylation by CBP and HIPK2, respectively.[15,16] The association of these bodies with ubiquitination and subunits of the 20S proteasome also implicate these subnuclear domains in regulating protein turn-over, including the PML protein itself.[68-70] Thus, it has become increasingly clear that rather than just sequestering proteins, PML NBs also serve as cellular nodes that may facilitate diverse nuclear functions by acting as catalytic surfaces to enhance the association of nuclear proteins with their modifying enzymes.[3,4] As such, PML NBs could enable efficient DNA damage signaling and repair by a number of mechanisms including the sequestration and release of important DNA repair factors such as ATR and TopBP1,[20,21] the co-recruitment of post-translational modification of proteins such as p53 and MRE11,[15,16,31] and by promoting the phosphorylation and activation of checkpoint kinases such as Chk2.[18]

If PML NBs do indeed serve as catalytic surfaces for the post-translational modification of nuclear proteins, then changes in biochemical composition, size and number of these bodies may play an important role in modulating the "intensity" of DNA damage signaling to physiological or therapeutic levels of DNA damage. This paradigm is not a new one, as other proteins can similarly modulate the DNA repair response to physiological levels of DNA damage such as NBS1, which is required for efficient activation of Chk2 kinase by low levels of ionizing radiation.[71] We demonstrated previously that PML NBs increase in number in response to DNA DSBs through a fission process, where new and smaller bodies arise from pre-existing PML NBs.[25] Most importantly, the new PML NBs arising by fission appear to share the same biochemical composition as the "parental" bodies from which they arose. Similarly, we found that PML NB protein composition was identical between Mock and KAP1 depleted NHDFs even though body number had increased overall (data not shown). As such even though PML NB number has increased, each body should retain the same ability to recruit or associate with DNA repair factors either directly by binding PML or indirectly by binding various PML NB-associated proteins such as SP100, which can recruit NBS1 to PML NBs.[72] This is in contrast to the disruption and redistribution of PML NBs into "thread-like" structures and/or smaller bodies with altered biochemical composition by viral proteins expressed by a number of DNA tumor viruses, including human papilloma virus (HPV); herpes simplex virus (HSV), epstein barr (EBV) and adenovirus.[73-75] Interestingly, the disruption of PML NBs under these circumstances can also impair DNA damage signaling and apoptosis, as recently demonstrated for the EBV protein EBNA1.[75] The process of PML NB fission effectively subdivides the PML NBs into smaller structures that have a larger relative surface area to their volume with identical biochemical composition. Thus, we hypothesize that the "state-of-subdivision" of PML NBs after genotoxic stress is directly proportional to the total surface area available for NB-associated proteins involved in DNA damage signaling and repair to interact with the enzymes that post-translationally modify them. The current study now implicates KAP1 as a possible mediator of ATM-dependent changes in PML NB number, most likely by altering the organization and density of cellular chromatin in response to DNA DSBs. Although the "state-of-subdivision" model is highly speculative, it does provide one possible experimental paradigm for future studies in the role of PML NBs in the cellular response to DNA damage.

Materials and Methods

Chemical reagents. Unless otherwise stated all chemical reagents were purchased from Sigma Aldrich.

Cell lines and drug treatments. Cell lines used in this study are as follows: Phoenix helper-free retrovirus producer cell line (gift from C. McCormick, Dalhousie University); normal human diploid fibroblasts (NHDF) (GM05757; Coriell Cell Repository); and osteosarcoma (U2-OS) cells expressing short hairpin RNA (shRNA) against GFP or KAP1.[35] Phoenix and U2-OS cells were grown in Dulbecco's modified eagle medium (DMEM) supplemented with 10% fetal bovine serum (FBS) and 1% penicillin-streptomycin solution. U2-OS cells expressing GFP or KAP1 shRNA were grown in complete medium supplemented with 1 μg/mL puromycin. NHDF and subsequent Tert-immortalized

cell lines derived from them (5757-TERT) were grown in alpha-minimum essential medium eagle (α-MEME) supplemented with 15% FBS and 1% penicillin-streptomycin-glutamine solution. All cell lines were cultured at 37°C in a 5% CO_2 atmosphere. To induce DSBs, cells were treated with 20 μM etoposide (VP16) for 30 min, washed in phosphate-buffered saline (PBS) twice (WISENT Inc.) and left to recover for the indicated periods of time. For ATM inhibition, cells were incubated for 30 min in growth medium containing 10 μM KU55933, a specific inhibitor of ATM[45] prior to induction of DNA damage with etoposide, and maintained in growth medium containing 10 μM KU55933 as cells recovered from etoposide for the indicated times. For histone deacetylase (HDAC) inhibition experiments, cells were treated with 200 ng/ml of TSA (Sigma) for 4–6 h prior to fixation and processing for western blot or immunofluorescence analysis.

Generation of cell lines used in this study. All retroviral vectors were transfected into Phoenix cells using the Calcium Phosphate ProFection® Mammalian Transfection System (Promega), as described by the manufacturer. First a Tert immortalized NHDF cell line (5757-TERT) was generated by retroviral transduction of an early passage of NHDF (GM05757) using a pBabe-Hygro-hTert vector (Addgene; Counter et al. 1998) encoding the catalytic subunit of telomerase, followed by selection in 75 ug/mL hygromycin (BioShop). 5757-TERT cell lines stably expressing GFP shRNA or KAP1 shRNA were created through retroviral transduction of 5757-TERT cells using pRetrosuper-Puro vectors encoding shRNA against GFP or KAP1 respectively, followed by selection in 1 ug/mL puromycin as previously described in reference 35. 5757-TERT KAP1 shRNA cell lines (ΔKAP1) stably expressing wild-type or mutant KAP1 were created by retroviral transduction with the vector pCLXSN expressing HA-tagged wild-type KAP1, mutant KAP1 S824A or KAP1 S824D, respectively, and underwent selection with 1 ug/mL puromycin and 200 ug/mL neomycin.[35] At least two biological replicates of each of the cell lines produced were used for further analysis.

Immunofluorescence microscopy and statistical analysis of PML NB number. Cells were treated with or without etoposide to induced DSBs prior to fixation at the indicated time points and processing for immunofluorescence as previously described in reference 25. Cells were then blocked in 5% normal donkey serum (Sigma) in PBS before immunolabeling with the following primary antibodies: rabbit anti-PML (1:300) (Santa Cruz Biotech; SC-5621), rabbit anti-pan acetyl histone H4 (1:200) (Millipore; 06-598) or mouse anti-KRIP1 for KAP1 (1:500) (BD Biosciences; 610680). The secondary antibodies used were: anti-rabbit or anti-mouse antibodies conjugated to Alexa Fluor 488 (1:200) (A21206) or Alexa Fluor 568 (1:200) (A10037) (Invitrogen). Coverslips were then mounted in Vectashield antifade medium (Vector Laboratories, Inc.) containing 4,6' diamidino-2-phenylindole (DAPI) prior to microscopy.

Fluorescence images were taken using a 40x 1.4 NA oil-immersion objective lens on a Zeiss Axioplan 2 motorized upright fluorescence microscope fitted with a Zeiss Axiocam HRc digital camera. Images were acquired using AxioVision 4.6 (Zeiss). Further image processing and analysis was done using ImageJ v.1.42 (National Institutes for Health) (NIH) and Photoshop 8.0 (Adobe).

PML NB number was determined for 30 cells per time point for each experiment from maximum intensity Z-projections from multiple focal planes taken for each field of view using Image J v1.42 (NIH) and Excel (Microsoft), which were normalized using nucleus size as previously described in reference 25. Experiments were repeated in triplicate (n = 90 cells) for each cell line, and two biological replicates per cell line where analyzed where indicated to account for clonal artifacts. Error analysis was then expressed as standard error of the mean (SEM). Statistical significance between datasets was determined using the Student's t-test in Excel (Microsoft).

Western blot analysis. Whole cell lysates were prepared before and after etoposide treatment of cell lines by direct lysis of cells in 2x SDS loading buffer [20% glycerol, 125 mM Tris-HCl pH 6.8, 4% sodium dodecyl sulfate (SDS), 0.2% bromophenol blue, 10% β-mercaptoethanol] supplemented with 1x Protease Inhibitor Cocktail (Sigma) and the phosphatase inhibitors NaF (10 mM) and β-glycerolphosphate (40 mM). Lysates where then subjected to SDS-polyacrylamide gel electrophoresis (PAGE) and semi-dry transfer (BioRad) to polyvinylidene difluoride (PVDF) membrane, prior to detection with primary and secondary antibodies diluted in 5% milk/PBST. Western blots were developed using an ECL detection kit (Pierce). Primary antibodies used were: KAP1 (BD Biosciences; 610680), phosphorylated Ser 824 on KAP1 (Bethyl Laboratories, Inc., A300-767A), ATM (Abcam; ab17995), phosphorylated Ser 1981 on ATM (Abcam; ab36810), phophorylated Ser 139 on γ-H2A.X (Millipore; 05-636), pan-acetylated histone H4 (Millipore, 06-598), β-tubulin (Santa Cruz, sc-9104) and β-actin (Sigma; A2228). Secondary antibodies used were: anti-mouse (A6782) or anti-rabbit (A6154) horseradish peroxidase (Sigma).

Flow cytometry and cell cycle analysis. Cells were pelleted by centrifugation at 4,000 rpm for 5 min, washed in cold PBS and fixed in 70% ethanol at -20°C overnight. Before FACS analysis, cells were again pelleted, washed in PBS containing 0.2 mg/mL RNase, and following centrifugation (as above) resuspended in PBS-RNase containing 50 μg/mL propidium iodide to a final cell concentration of 3 x 10^6 cells/mL. The cells were then kept on ice for 30 min prior to analysis using a FACSCalibur flow cytometer (BD Biosciences). Cell profiles were then determined from FACS data using Modfit LT 3.0 software (Verity). FACS experiments were done in triplicate for at each cell line and the the percentage of cells in each cell cycle phase was represented as an average value for single cell lines or between biological replicates as indicated.

Electron spectroscopic imaging (ESI) and statistical analysis of chromatin density. Control (Mock) and ΔKAP1 5757-TERT NHDFs were grown to 100% confluence on coverslips to enrich for G_0/G_1 cells and directly fixed in 4% paraformaldehyde (EMS) for 10 min at room temperature (RT) before being permeabilized in PBS containing 0.5% Triton X-100 for 5 min, post fixed in 1% glutaraldehyde (EMS) for 5 min at RT. The cells were then dehydrated in an ethanol series and embeded in Quetol 651

(EMS) before being processed, sectioned and imaged by ESI as previously described in reference 51, using a Tecnai 20 transmission electron microscope (FEI) equipped with an energy-filtering spectrometer (Gatan). Energy-filtered electron micrographs of nitrogen (N) and phosphorus (P) were collected, and non-chromosomal protein was segmented by subtracting the N from the P ESI micrograph, which was then false colored in cyan and combined in a composite image with the P ESI micrograph false colored in yellow in Photoshop 11.0 (Adobe) to highlight chromatin. The composite elemental maps of N-P (cyan) and P (yellow) were then analyzed for thickness of nuclear-lamina-associated chromatin using Image J v1.42 software (NIH). Pixel measurements (n = 50 measurements taken from 5 cells) were converted into microns (μm) and then averaged. Statistical significance between cell lines was generated using the Student's t-test in Excel (Microsoft).

For the statistical analysis of chromatin density, chromatin was first segmented within composite ESI micrographs of Mock and ΔKAP1 5757-TERT NHDFs as previously described in reference 27. Briefly, the N and P ESI micrographs were first false colored in green and red, respectively, and combined into a single RGB image using Photoshop 11.0 (Adobe). In the merged image chromatin becomes apparent as yellow 10 nm and higher-order fibers. These images were then imported into ImageJ v1.42 (NIH) and the Color Threshold Plugin (Gabriel Landini) was used to segment only those yellow pixels that morphologically resemble chromatin. The thresholded image was then converted to an 8-bit grayscale image and the Threshold tool in ImageJ was used to create a binary mask representing only chromatin and areas determined using the Particle Picker tool in ImageJ. The percentage area was then defined as the ratio of the area of chromatin divided by the total area of the image in square pixels. The percentage density measurements were then averaged (n = 50 measurements taken from 5 cells) and statistical significance between datasets was generated using the Student's t-test in Excel (Microsoft).

Acknowledgements

G.D. is a Canadian Institutes of Health Research (CIHR) New Investigator and the Cameron Research Scientist of the Dalhousie University Cancer Research Program. Y.S. is an Israel Cancer Research Fund Research Professor. R.K. was a recipient of a Killam Predoctoral Fellowship and K.A. is supported by a trainee award from The Beatrice Hunter Cancer Research Institute with funds provided by The Terry Fox Foundation Strategic Health Research Training Program in Cancer Research at the CIHR. This work was funded by an operating grant awarded to G.D. from the Canadian Institutes of Health Research (MOP-84260). Work in the laboratory of Y.S. is funded by the A-T Medical Research Foundation and the Israel Cancer Research Fund.

Note

Supplemental materials can be found at:
www.landesbioscience.com/journals/cc/article/14551

References

1. Charames GS, Bapat B. Genomic instability and cancer. Curr Mol Med 2003; 3:589-96; PMID: 14601634.
2. Negrini S, Gorgoulis VG, Halazonetis TD. Genomic instability—an evolving hallmark of cancer. Nat Rev Mol Cell Biol 2010; 11:220-8; PMID: 20177397; DOI: 10.1038/nrm2858.
3. Bernardi R, Pandolfi PP. Structure, dynamics and functions of promyelocytic leukaemia nuclear bodies. Nat Rev Mol Cell Biol 2007; 8:1006-16; PMID: 17928811; DOI: 10.1038/nrm2277.
4. Dellaire G, Bazett-Jones DP. PML nuclear bodies: dynamic sensors of DNA damage and cellular stress. Bioessays 2004; 26:963-77; PMID: 15351967; DOI: 10.1002/bies.20089.
5. Salomoni P, Pandolfi PP. The role of PML in tumor suppression. Cell 2002; 108:165-70; PMID: 11832207; DOI: S0092867402006268.
6. Dyck JA, Maul GG, Miller WH Jr, Chen JD, Kakizuka A, Evans RM. A novel macromolecular structure is a target of the promyelocyte-retinoic acid receptor oncoprotein. Cell 1994; 76:333-43; PMID: 8293467; DOI: 0092-8674(94)90340-9.
7. Koken MH, Puvion-Dutilleul F, Guillemin MC, Viron A, Linares-Cruz G, Stuurman N, et al. The t(15;17) translocation alters a nuclear body in a retinoic acid-reversible fashion. EMBO J 1994; 13:1073-83; PMID: 8131741.
8. Gurrieri C, Capodieci P, Bernardi R, Scaglioni PP, Nafa K, Rush LJ, et al. Loss of the tumor suppressor PML in human cancers of multiple histologic origins. J Natl Cancer Inst 2004; 96:269-79; PMID: 14970276; DOI: 10.1093/jnci/djh043.
9. Scaglioni PP, Yung TM, Cai LF, Erdjument-Bromage H, Kaufman AJ, Singh B, et al. A CK2-dependent mechanism for degradation of the PML tumor suppressor. Cell 2006; 126:269-83; PMID: 16873060; DOI: 10.1016/j.cell.2006.05.041.
10. Trotman LC, Alimonti A, Scaglioni PP, Koutcher JA, Cordon-Cardo C, Pandolfi PP. Identification of a tumor suppressor network opposing nuclear Akt function. Nature 2006; 441:523-7; PMID: 16680151; DOI: 10.1038/nature04809.
11. Zhong S, Hu P, Ye TZ, Stan R, Ellis NA, Pandolfi PP. A role for PML and the nuclear body in genomic stability. Oncogene 1999; 18:7941-7; PMID:10637504; DOI: 10.1038/sj.onc.1203367.
12. Guo A, Salomoni P, Luo J, Shih A, Zhong S, Gu W, et al. The function of PML in p53-dependent apoptosis. Nat Cell Biol 2000; 2:730-6; PMID:11025664; DOI: 10.1038/35036365.
13. Fogal V, Gostissa M, Sandy P, Zacchi P, Sternsdorf T, Jensen K, et al. Regulation of p53 activity in nuclear bodies by a specific PML isoform. EMBO J 2000; 19:6185-95; PMID:11080164; DOI: 10.1093/emboj/19.22.6185.
14. Wang ZG, Delva L, Gaboli M, Rivi R, Giorgio M, Cordon-Cardo C, et al. Role of PML in cell growth and the retinoic acid pathway. Science 1998; 279:1547-51; PMID: 9488655; DOI: 10.1126/science.279.5356.1547.
15. Hofmann TG, Moller A, Sirma H, Zentgraf H, Taya Y, Droge W, et al. Regulation of p53 activity by its interaction with homeodomain-interacting protein kinase-2. Nat Cell Biol 2002; 4:1-10; PMID: 11740489; DOI: 10.1038/ncb715.
16. D'Orazi G, Cecchinelli B, Bruno T, Manni I, Higashimoto Y, Saito S, et al. Homeodomain-interacting protein kinase-2 phosphorylates p53 at Ser 46 and mediates apoptosis. Nat Cell Biol 2002; 4:11-9; PMID: 11780126; DOI: 10.1038/ncb714.
17. Yang S, Kuo C, Bisi JE, Kim MK. PML-dependent apoptosis after DNA damage is regulated by the checkpoint kinase hCds1/Chk2. Nat Cell Biol 2002; 4:865-70; PMID: 12402044; DOI: 10.1038/ncb869.
18. Yang S, Jeong JH, Brown AL, Lee CH, Pandolfi PP, Chung JH, et al. Promyelocytic leukemia activates Chk2 by mediating Chk2 autophosphorylation. J Biol Chem 2006; 281:26645-54; PMID:16835227; DOI: 10.1074/jbc.M604391200.
19. Boisvert FM, Hendzel MJ, Masson JY, Richard S. Methylation of MRE11 regulates its nuclear compartmentalization. Cell Cycle 2005; 4:981-9; PMID:15970667.
20. Xu ZX, Timanova-Atanasova A, Zhao RX, Chang KS. PML colocalizes with and stabilizes the DNA damage response protein TopBP1. Mol Cell Biol 2003; 23:4247-56; PMID: 12773567; DOI: 10.1128/MCB.23.12.4247-56.2003.
21. Barr SM, Leung CG, Chang EE, Cimprich KA. ATR kinase activity regulates the intranuclear translocation of ATR and RPA following ionizing radiation. Curr Biol 2003; 13:1047-51; PMID: 12814551; DOI: S0960982203003762.
22. Boe SO, Haave M, Jul-Larsen A, Grudic A, Bjerkvig R, Lonning PE. Promyelocytic leukemia nuclear bodies are predetermined processing sites for damaged DNA. J Cell Sci 2006; 119:3284-95; PMID: 16868026; DOI: 10.1242/jcs.03068.
23. Yeager TR, Neumann AA, Englezou A, Huschtscha LI, Noble JR, Reddel RR. Telomerase-negative immortalized human cells contain a novel type of promyelocytic leukemia (PML) body. Cancer Res 1999; 59:4175-9; PMID: 10485449.
24. Carbone R, Pearson M, Minucci S, Pelicci PG. PML NBs associate with the hMre11 complex and p53 at sites of irradiation induced DNA damage. Oncogene 2002; 21:1633-40; PMID: 11896594; DOI: 10.1038/sj.onc.1205227.

25. Dellaire G, Ching RW, Ahmed K, Jalali F, Tse KC, Bristow RG, et al. Promyelocytic leukemia nuclear bodies behave as DNA damage sensors whose response to DNA double-strand breaks is regulated by NBS1 and the kinases ATM, Chk2 and ATR. J Cell Biol 2006; 175:55-66; PMID:17030982; DOI: 10.1083/jcb.200604009.
26. Varadaraj A, Dovey CL, Laredj L, Ferguson B, Alexander CE, Lubben N, et al. Evidence for the receipt of DNA damage stimuli by PML nuclear domains. J Pathol 2007; 211:471-80; PMID: 17206596; DOI: 10.1002/path.2126.
27. Dellaire G, Kepkay R, Bazett-Jones DP. High resolution imaging of changes in the structure and spatial organization of chromatin, gamma-H2A.X and the MRN complex within etoposide-induced DNA repair foci. Cell Cycle 2009; 8:3750-69; PMID: 19855159; DOI: 10.4161/cc.8.22.10065.
28. Kurki S, Latonen L, Laiho M. Cellular stress and DNA damage invoke temporally distinct Mdm2, p53 and PML complexes and damage-specific nuclear relocalization. J Cell Sci 2003; 116:3917-25; PMID:12915590; DOI: 10.1242/jcs.00714.
29. Shiloh Y. ATM and related protein kinases: safeguarding genome integrity. Nat Rev Cancer 2003; 3:155-68; PMID: 12612651; DOI: 10.1038/nrc1011.
30. Kurz EU, Lees-Miller SP. DNA damage-induced activation of ATM and ATM-dependent signaling pathways. DNA Repair (Amst) 2004; 3:889-900; PMID: 15279774; DOI: 10.1016/j.dnarep.2004.03.029.
31. Boisvert FM, Hendzel MJ, Bazett-Jones DP. Promyelocytic leukemia (PML) nuclear bodies are protein structures that do not accumulate RNA. J Cell Biol 2000; 148:283-92; PMID: 10648561; 10.1083/jcb.148.2.283.
32. Pandita TK, Richardson C. Chromatin remodeling finds its place in the DNA double-strand break response. Nucleic Acids Res 2009; 37:1363-77; PMID: 19139074; DOI: 10.1093/nar/gkn1071.
33. Misteli T, Soutoglou E. The emerging role of nuclear architecture in DNA repair and genome maintenance. Nat Rev Mol Cell Biol 2009; 10:243-54; PMID: 19277046; DOI: 10.1038/nrm2651.
34. van AH, Gasser SM. Crosstalk between histone modifications during the DNA damage response. Trends Cell Biol 2009; 19:207-17; PMID: 19342239; DOI: 10.1016/j.tcb.2009.03.001.
35. Ziv Y, Bielopolski D, Galanty Y, Lukas C, Taya Y, Schultz DC, et al. Chromatin relaxation in response to DNA double-strand breaks is modulated by a novel ATM- and KAP-1 dependent pathway. Nat Cell Biol 2006; 8:870-6; PMID: 16862143; DOI: 10.1038/ncb1446.
36. Kruhlak MJ, Celeste A, Dellaire G, Fernandez-Capetillo O, Muller WG, McNally JG, et al. Changes in chromatin structure and mobility in living cells at sites of DNA double-strand breaks. J Cell Biol 2006; 172:823-34; PMID: 16520385; DOI: 10.1083/jcb.200510015.
37. Ju R, Muller MT. Histone deacetylase inhibitors activate p21(WAF1) expression via ATM. Cancer Res 2003; 63:2891-7; PMID: 12782595.
38. Bakkenist CJ, Kastan MB. DNA damage activates ATM through intermolecular autophosphorylation and dimer dissociation. Nature 2003; 421:499-506; PMID: 12556884; DOI: 10.1038/nature01368.
39. Ryan RF, Schultz DC, Ayyanathan K, Singh PB, Friedman JR, Fredericks WJ, et al. KAP-1 corepressor protein interacts and colocalizes with heterochromatic and euchromatic HP1 proteins: a potential role for Kruppel-associated box-zinc finger proteins in heterochromatin-mediated gene silencing. Mol Cell Biol 1999; 19:4366-78; PMID: 10330177.
40. O'Geen H, Squazzo SL, Iyengar S, Blahnik K, Rinn JL, Chang HY, et al. Genome-wide analysis of KAP1 binding suggests autoregulation of KRAB-ZNFs. PLoS Genet 2007; 3:89; PMID: 17542650; DOI: 10.1371/journal.pgen.0030089.
41. Friedman JR, Fredericks WJ, Jensen DE, Speicher DW, Huang XP, Neilson EG, et al. KAP-1, a novel corepressor for the highly conserved KRAB repression domain. Genes Dev 1996; 10:2067-78; PMID: 8769649; DOI: 10.1101/gad.10.16.2067.
42. Goodarzi AA, Noon AT, Deckbar D, Ziv Y, Shiloh Y, Lobrich M, et al. ATM signaling facilitates repair of DNA double-strand breaks associated with heterochromatin. Mol Cell 2008; 31:167-77; PMID: 18657500; DOI: 10.1016/j.molcel.2008.05.017.
43. White DE, Negorev D, Peng H, Ivanov AV, Maul GG, Rauscher FJ, III. KAP1, a novel substrate for PIKK family members, colocalizes with numerous damage response factors at DNA lesions. Cancer Res 2006; 66:11594-9; PMID: 17178852; DOI: 10.1158/0008-5472.CAN-06-4138.
44. Noon AT, Shibata A, Rief N, Lobrich M, Stewart GS, Jeggo PA, et al. 53BP1-dependent robust localized KAP-1 phosphorylation is essential for heterochromatic DNA double-strand break repair. Nat Cell Biol 2010; 12:177-84; PMID: 20081839; DOI: 10.1038/ncb2017.
45. Hickson I, Zhao Y, Richardson CJ, Green SJ, Martin NM, Orr AI, et al. Identification and characterization of a novel and specific inhibitor of the ataxia-telangiectasia mutated kinase ATM. Cancer Res 2004; 64:9152-9; PMID: 15604286; DOI: 10.1158/0008-5472.CAN-04-2727.
46. Goodarzi AA, Noon AT, Jeggo PA. The impact of heterochromatin on DSB repair. Biochem Soc Trans 2009; 37:569-76; PMID: 19442252; DOI: 10.1042/BST0370569.
47. Dellaire G, Ching RW, Dehghani H, Ren Y, Bazett-Jones DP. The number of PML nuclear bodies increases in early S phase by a fission mechanism. J Cell Sci 2006; 119:1026-33; PMID: 16492708; DOI: 10.1242/jcs.02816.
48. Eskiw CH, Dellaire G, Bazett-Jones DP. Chromatin contributes to structural integrity of promyelocytic leukemia bodies through a SUMO-1-independent mechanism. J Biol Chem 2004; 279:9577-85; PMID: 14672938; DOI: 10.1074/jbc.M312580200.
49. Bryan TM, Englezou A, Dalla-Pozza L, Dunham MA, Reddel RR. Evidence for an alternative mechanism for maintaining telomere length in human tumors and tumor-derived cell lines. Nat Med 1997; 3:1271-4; PMID: 9359704; DOI: 10.1038/nm1197-271.
50. Terris B, Baldin V, Dubois S, Degott C, Flejou JF, Henin D, et al. PML nuclear bodies are general targets for inflammation and cell proliferation. Cancer Res 1995; 55:1590-7; PMID: 7882370.
51. Koken MH, Linares-Cruz G, Quignon F, Viron A, Chelbi-Alix MK, Sobczak-Thepot J, et al. The PML growth-suppressor has an altered expression in human oncogenesis. Oncogene 1995; 10:1315-24; PMID: 7731682.
52. Dellaire G, Nisman R, Bazett-Jones DP. Correlative light and electron spectroscopic imaging of chromatin in situ. Methods Enzymol 2004; 375:456-78; PMID: 14870683.
53. Nielsen AL, Ortiz JA, You J, Oulad-Abdelghani M, Khechumian R, Gansmuller A, et al. Interaction with members of the heterochromatin protein 1 (HP1) family and histone deacetylation are differentially involved in transcriptional silencing by members of the TIF1 family. EMBO J 1999; 18:6385-95; PMID: 10562550; DOI: 10.1093/emboj/18.22.6385.
54. Schultz DC, Ayyanathan K, Negorev D, Maul GG, Rauscher FJ, III. SETDB1: a novel KAP-1-associated histone H3, lysine 9-specific methyltransferase that contributes to HP1-mediated silencing of euchromatic genes by KRAB zinc-finger proteins. Genes Dev 2002; 16:919-32; PMID: 11959841; DOI: 10.1101/gad.973302.
55. Haaf T, Schmid M. Chromosome topology in mammalian interphase nuclei. Exp Cell Res 1991; 192:325-32; PMID: 1988281.
56. Murr R, Loizou JI, Yang YG, Cuenin C, Li H, Wang ZQ, et al. Histone acetylation by Trrap-Tip60 modulates loading of repair proteins and repair of DNA double-strand breaks. Nat Cell Biol 2006; 8:91-9; PMID: 16341205; DOI: 10.1038/ncb1343.
57. Ikura T, Ogryzko VV, Grigoriev M, Groisman R, Wang J, Horikoshi M, et al. Involvement of the TIP60 histone acetylase complex in DNA repair and apoptosis. Cell 2000; 102:463-73; PMID: 10966108; DOI: S0092-8674(00)00051-9.
58. Squatrito M, Gorrini C, Amati B. Tip60 in DNA damage response and growth control: many tricks in one HAT. Trends Cell Biol 2006; 16:433-42; PMID: 16904321; DOI: 10.1016/j.tcb.2006.07.007.
59. Toth KF, Knoch TA, Wachsmuth M, Frank-Stohr M, Stohr M, Bacher CP, et al. Trichostatin A-induced histone acetylation causes decondensation of interphase chromatin. J Cell Sci 2004; 117:4277-87; PMID: 15292402; DOI: 10.1242/jcs.01293.
60. Condemine W, Takahashi Y, Zhu J, Puvion-Dutilleul F, Guegan S, Janin A, de Thé H. Characterization of endogenous human promyelocytic leukemia isoforms. Cancer Res 2006; 66:6192-8; PMID: 16778193; DOI: 10.1158/0008-5472.CAN-05-3792.
61. Dehghani H, Dellaire G, Bazett-Jones DP. Organization of chromatin in the interphase mammalian cell. Micron 2005; 36:95-108; PMID: 15629642; DOI: 10.1016/j.micron.2004.10.003.
62. Jakobsson J, Cordero MI, Bisaz R, Groner AC, Busskamp V, Bensadoun JC, et al. KAP1-mediated epigenetic repression in the forebrain modulates behavioral vulnerability to stress. Neuron 2008; 60:818-31; PMID: 19081377; DOI: 10.1016/j.neuron.2008.09.036.
63. Rowe HM, Jakobsson J, Mesnard D, Rougemont J, Reynard S, Aktas T, et al. KAP1 controls endogenous retroviruses in embryonic stem cells. Nature 2010; 463:237-40; PMID: 20075919; DOI: 10.1038/nature08674.
64. Negorev D, Maul GG. Cellular proteins localized at and interacting within ND10/PML nuclear bodies/PODs suggest functions of a nuclear depot. Oncogene 2001; 20:7234-42; PMID: 11704851; DOI: 10.1038/sj.onc.1204764.
65. Li H, Leo C, Zhu J, Wu X, O'Neil J, Park EJ, et al. Sequestration and inhibition of Daxx-mediated transcriptional repression by PML. Mol Cell Biol 2000; 20:1784-96; PMID: 10669754.
66. Ishov AM, Sotnikov AG, Negorev D, Vladimirova OV, Neff N, Kamitani T, et al. PML is critical for ND10 formation and recruits the PML-interacting protein daxx to this nuclear structure when modified by SUMO-1. J Cell Biol 1999; 147:221-34; PMID: 10525530.
67. LaMorte VJ, Dyck JA, Ochs RL, Evans RM. Localization of nascent RNA and CREB binding protein with the PML-containing nuclear body. Proc Natl Acad Sci USA 1998; 95:4991-6; PMID: 9560216.
68. Mattsson K, Pokrovskaja K, Kiss C, Klein G, Szekely L. Proteins associated with the promyelocytic leukemia gene product (PML)-containing nuclear body move to the nucleolus upon inhibition of proteasome-dependent protein degradation. Proc Natl Acad Sci USA 2001; 98:1012-7; PMID: 11158586; DOI: 10.1073/pnas.031566998.
69. Tatham MH, Geoffroy MC, Shen L, Plechanovova A, Hattersley N, Jaffray EG, et al. RNF4 is a poly-SUMO-specific E3 ubiquitin ligase required for arsenic-induced PML degradation. Nat Cell Biol 2008; 10:538-46; PMID: 18408734; DOI: 10.1038/ncb1716.
70. Lallemand-Breitenbach V, Jeanne M, Benhenda S, Nasr R, Lei M, Peres L, et al. Arsenic degrades PML or PML-RARalpha through a SUMO-triggered RNF4/ubiquitin-mediated pathway. Nat Cell Biol 2008; 10:547-55; PMID: 18408733; DOI: 10.1038/ncb1717.

71. Buscemi G, Savio C, Zannini L, Micciche F, Masnada D, Nakanishi M, et al. Chk2 activation dependence on Nbs1 after DNA damage. Mol Cell Biol 2001; 21:5214-22; PMID: 11438675; DOI: 10.1128/MCB.21.15.5214-22.2001.
72. Naka K, Ikeda K, Motoyama N. Recruitment of NBS1 into PML oncogenic domains via interaction with SP100 protein. Biochem Biophys Res Commun 2002; 299:863-71; PMID:12470659; DOI: S0006291X02027559.
73. Everett RD. DNA viruses and viral proteins that interact with PML nuclear bodies. Oncogene 2001; 20:7266-73; PMID: 11704855; DOI: 10.1038/sj.onc.1204759.
74. Everett RD. Interactions between DNA viruses, ND10 and the DNA damage response. Cell Microbiol 2006; 8:365-74; PMID: 16469050; DOI: 10.1111/j.1462-5822.2005.00677.x.
75. Sivachandran N, Sarkari F, Frappier L. Epstein-Barr nuclear antigen 1 contributes to nasopharyngeal carcinoma through disruption of PML nuclear bodies. PLoS Pathog 2008; 4:1000170; PMID: 18833293; DOI: 10.1371/journal.ppat.1000170.